Modification of Chitosan-Coated Magnetic Material with Glycidyl-trimethylammonium Chloride for Cr(VI) Adsorption

Salwa Kamilia, Feri Mukhayani, Sutarno Sutarno, and Nuryono Nuryono*

Department of Chemistry, Faculty of Mathematics and Natural Sciences, Universitas Gadjah Mada, Sekip Utara, Yogyakarta 55281, Indonesia

*** Corresponding author:**

email: nuryono_mipa@ugm.ac.id

Received: October 16, 2024
Accepted: November 26, 2024

DOI: 10.22146/ijc.100749

Abstract: *Modification of chitosan-coated magnetic material with quaternary ammonium chloride as adsorbent for Cr(VI) anions has been studied. The works included magnetic material (MM) separation from iron sand, magnetic material-chitosan (MM/Chit) synthesis, and attachment of quaternary ammonium groups from glycidyl trimethyl ammonium chloride (GTMAC) on MM/Chit to produce MM/Chit/GTMAC with various mass ratios. Products were characterized with FTIR, XRD, SEM-EDX, and VSM. Adsorption studies were carried out in a batch system with pH, time, and initial Cr(VI) concentration variations. The unadsorbed Cr(VI) was analyzed with AAS, and the adsorbed Cr(VI) was calculated from the difference between initial and unadsorbed concentrations of Cr(VI). The results showed that MM/Chit/GTMAC was successfully synthesized, and adding GTMAC increased the stability of MM/Chit and shifted the optimum pH for Cr(VI) adsorption from 3.0 to 4.0. The study of kinetics and adsorption isotherm showed that the adsorption of Cr(VI) anion on the adsorbent MM/Chit/GTMAC (with the mass ratio of Chit to GTMAC 1:6) follows the pseudo-second-order kinetic model with the adsorption rate constant of 5.3 × 10^{-3} g mg^{-1} min^{-1} and Langmuir isotherms with the adsorption maximum capacity of 104.17 mg g^{-1}, which has a potential to be applied for removing Cr(VI) from polluted wastewater.*

Keywords: *chitosan; quaternary ammonium; chromium(VI); iron sand*

■ INTRODUCTION

Chromium (Cr) is one of the most toxic inorganic pollutants because it has many detrimental effects (mutagenic and carcinogenic) on human health and the environment [1]. The solubility and mobility of ionic species containing Cr(VI) are higher than Cr(III) [2]. In addition, it has been investigated that in an aqueous solution, the toxicity of Cr(VI) is 100 times more dangerous than Cr(III) [3]. There are many procedures that have been developed, such as adsorption [4], coagulation [5], membrane separation [6], photocatalytic degradation [7], and ion exchange [8], to remove Cr(VI) from aquatic environments. Each procedure has its advantages and disadvantages, depending on the application. However, these methods are costly when Cr(VI) is present at trace levels. Among them, the efficient method that has been proven to remove Cr(VI) is adsorption. It has several advantages, i.e., high efficiency, economically feasible, environmentally friendly, and ease of regeneration [9].

Adsorbent for removal of Cr(VI) could be regenerated from low-cost biomass as starting materials such as lignin [10], chitosan [11], alginate [12], and cellulose [13]. Chitosan is widely used in the adsorption process. Chitosan contains polar groups of $–NH_2$ and –OH. They have excellent adsorption capacity for anionic metal and have received more attention to be functionalized [14]. Chitosan has good non-toxicity, biocompatibility, biodegradability, low cost, and high adsorption capacity [15]. Several chemical modifications have been performed, including quaternization [16], crosslinking [17], and new functional group insertion [18] to improve chitosan stability and adsorption capacity. Quaternization can be chosen as an excellent

technique to modify chitosan since the quaternized polymers usually promote the adsorption ability. They are positively charged after quaternization and suitable for adsorbent of anions.

Glycidyl-trimethylammonium chloride (GTMAC), a low-toxic quaternary ammonium salt [19], is usually chosen to quaternate chitosan to increase its adsorption capacity of anions. The reaction between chitosan and GTMAC is affected by pH. Under acidic and neutral conditions, the –OH group of chitosan is weak to open the epoxide ring of GTMAC, and only the $–NH_2$ group of chitosan is strong enough to attack the epoxide ring of GTMAC. On the other hand, in basic conditions, both $–NH_2$ and –OH groups of chitosan can react with GTMAC, forming covalent bonding by the epoxide ring opening of GTMAC [20]. Magnetic material (MM) is introduced to quaternary ammonium-modified chitosan to simplify the adsorbent separation. Moreover, MM also exhibits high mechanical strength in the modified material [21].

In this paper, we report the modification of chitosan-coated MM with GTMAC to obtain an adsorbent with high stability and Cr(VI) adsorption capacity. The Cr(VI) adsorption on MM/chitosan/GTMAC was performed in a batch system with various pH, time adsorption, and initial Cr(VI) concentrations. Then, kinetics and adsorption isotherm parameters are determined and evaluated using appropriate models.

■ EXPERIMENTAL SECTION

Materials

Iron sands were collected from Glagah Beach, Kulon Progo, Yogyakarta. The chemicals used to produce MM/Chit/GTMAC included GTMAC ($C_6H_{14}ClNO$, 90% and density 1.13 g/mL), chitosan, acetic acid (CH_3COOH), hydrochloric acid (HCl), sulfuric acid (H_2SO_4), ammonium hydroxide (NH_4OH), sodium hydroxide (NaOH), and sodium chloride (NaCl). Cr(VI) solutions were prepared by dissolving potassium dichromate ($K_2Cr_2O_7$) in distilled water. All chemicals were purchased from Merck and used without any previous treatment.

Instrumentation

The apparatus used in this study for synthesis were laboratory glassware (Pyrex, Iwaki), hotplate completed with magnetic stirrer, mortar, analytical balance (Mettler Toledo, Shimadzu AUW120), oven (Memmert UN 55-53L), 200 mesh sieve, and universal pH (Merck). For characterization, several instruments were used, i.e., infrared spectrophotometer (Shimadzu FTIR Prestige-21), X-ray diffraction (XRD, Rigaku Multiplex, Cu source), scanning electron microscope-energy dispersive X-ray (SEM-EDX, Hitachi SU 3500), vibrating sample magnetometer (VSM, OXFORD 1.2T), UV-vis spectrophotometry (Shimadzu UV-1700 (E)), and atomic absorption spectrophotometer (AAS, Perkin Elmer 3110).

Procedure

Separation of MM

The MM separation followed the previous report with modification [18,22]. The iron sand sample (10 g) was washed with water repeatedly until the water was clear. Then, the washed-iron sand was dried under the sun for 48 h. After that, the MM was separated by using an external magnet. MM was grounded manually in a mortar and was sieved through a 200 mesh sieve. Next, MM (200 mesh) was washed with distilled water until the washing water was clear. The washed MM was dried in an oven at 90 °C for 18 h and stored in a bottle.

Preparation of MM/Chit/GTMAC composite

Typically, 0.15 g of chitosan was dissolved in 30 mL of CH_3COOH 1% until it forms a gel. Then, 0.5 g of activated MM was added to the prepared chitosan solution and stirred for 5 h at room temperature (25 °C). After the reaction finished, NH_4OH 0.5 M solution was added in drops to the mixture until pH 7. Then, GTMAC was added, and various masses of GTMAC were presented in Table 1. The composites were heated in an oven at 60 °C for 24 h. Next, the synthesized composites were characterized with FTIR, XRD, SEM-EDX, and VSM.

Table 1. The composition of MM, chitosan, and GTMAC to synthesize MM/Chit/GTMAC

MM (g)	Chitosan (g)	GTMAC (mL)	Codes
0.50	0.15	0.00	MM/Chit
		0.26	MM/Chit/GTMAC(1:2)
		0.53	MM/Chit/GTMAC(1:4)
		0.79	MM/Chit/GTMAC(1:6)

Characterization of MM/Chit/GTMAC

The IR spectra were recorded using a Nicolet 380 FTIR spectrometer in the 4000–400 cm^{-1} range. The diffraction pattern of the samples was analyzed on an XRD with Cu Kα characteristic radiation at a voltage of 40 kV and a current of 25 mA. The scanning rate was 5° min^{-1}, and the scanning scope of 2θ was from 10–80° at room temperature. SEM images were taken using a SEM JEOL-JCM 5700, and the composite elemental composition was calculated by using EDX. The magnetization value of the samples was measured using a SQUID-VSM magnetometer.

Determination of the point of zero charge (pH_{pzc})

Synthesized composite (20 mg) was mixed with 10 mL of NaCl solution 0.01 M, and the pH was adjusted in a range of 2, 3, 4, 5, 6, 7, 8, 9, and 10 using HCl and NaOH. The prepared mixtures were shaken for 2 h and kept in the dark for 48 h at room temperature. Then, the composite was separated with an external magnet, and the final pH of the solution was recorded. A similar work was performed without composite as the control. The pH_{pzc} was obtained from the intersection point of the composite solution and the control on the curve of final pH vs. initial pH.

Stability test of composites

Each of the composites (20 mg) was mixed with 10 mL of distilled water at various pH (1, 2, 3, 4, 5, 6, 7, 8, and 9). The mixtures were stirred for 2 h and then separated with an external magnet. The filtrate solutions were analyzed using AAS and UV-vis spectrometer. The Fe concentration in the filtrate was analyzed using AAS, and the soluble chitosan was analyzed using a UV-Vis spectrometer.

Adsorption

Adsorption of Cr(VI) was performed using batch method. Firstly, 20 mL of Cr(VI) 50 mg L^{-1} solution was mixed with 50 mg of adsorbent. The adsorption was carried out at room temperature for 2 h. The pH of the solution was adjusted at 1, 2, 3, 4, 5, 6, 7, 8, 9, and 10 using H_2SO_4 and NaOH. After the adsorption finished, the adsorbent was separated with an external magnet, and the Cr(VI) concentration after the adsorption was determined using AAS. Variations of contact time (10, 20, 30, 60, 90, 120, 150, and 180 min) and initial concentration of Cr(VI) (20, 50, 100, 150, 200, and 250 mg L^{-1}) were performed in this experiment. The kinetics model and adsorption isotherm were evaluated based on the adsorption data over the optimum MM/Chit/GTMAC adsorbent.

Table 2. Kinetics models

Model	Linear equation	Plot
Pseudo-first-order	$\ln\frac{q_e}{(q_e-q_t)}=k_1t$	$\ln\frac{q_e}{(q_e-q_t)}$ vs. t
Pseudo-second-order	$\frac{t}{q_t}=\frac{t}{q_e}+\frac{1}{k_2q_e^2}$	$\frac{t}{q_t}$ vs. t

Kinetics study

Adsorption kinetics was modeled using pseudo-first and pseudo-second-order rate laws with the formula summarized in Table 2.

Adsorption isotherm

The maximum adsorption capacity was calculated by applying the Freundlich and Langmuir adsorption models. The linear forms of these equations are given in Eq. (1) and (2) for the Langmuir isotherm model and Freundlich isotherm model, respectively;

$$\frac{C_e}{X_e}=\frac{C_l}{X_mK_L}+\frac{C_e}{X_m} \quad (1)$$

$$\log X_e=\log K_f+\frac{1}{n}\log C_e \quad (2)$$

where X_m and X_e are maximum, and equilibrium adsorption, C_e is equilibrium concentration, 1/n is heterogeneity factor, as well as K_L and K_f are Langmuir and Freundlich constants.

■ RESULTS AND DISCUSSION

Characteristics of MM/Chit/GTMAC

IR spectra

The FTIR spectra of MM in Fig. 1(a) show that there is a peak at 578 cm^{-1} corresponding to Fe–O stretching vibration. Coating chitosan on MM (Fig. 1(b)) leads to the appearance of chitosan characteristic peaks at 3423 cm^{-1} (O–H and N–H stretching vibrations), 2881 cm^{-1} (C–H stretching vibration), 1651 cm^{-1} (stretching C=O of amide I), 1550 cm^{-1} (–NH bending of amide II), 1419 cm^{-1} (–CH_2– bending vibration), 1377 cm^{-1} (–CH_3 symmetrical deformation of acetyl groups),

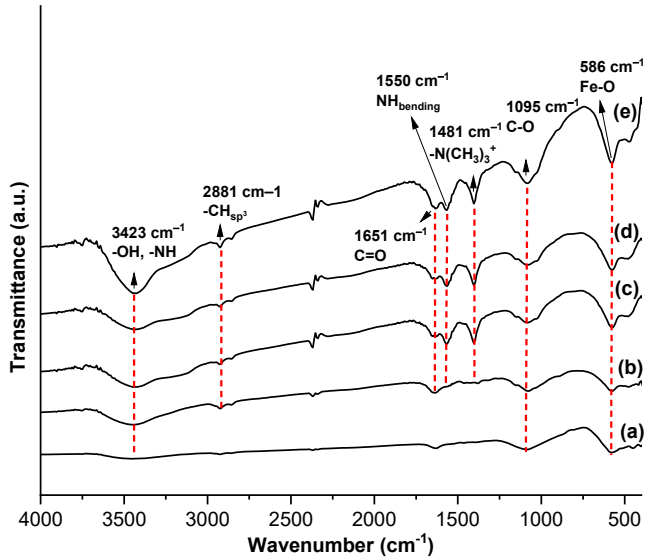

Fig 1. FTIR spectra of (a) MM, (b) MM/Chit, (c) MM/Chit/GTMAC(1:2), (d) MM/Chit/GTMAC(1:4), and (e) MM/Chit/GTMAC(1:6)

1151 cm^{-1} (asymmetric absorption of the C–O–C bridge), and 1080 cm^{-1} (C–O stretching vibration). These characteristic peaks agree with the IR spectra of chitosan in previous research [23]. In Fig. 1(c)-(e) for MM/Chit/GTMAC, there was a shift in the wavenumber from 3441 to 3425 cm^{-1} of $–NH_2$ group stretching vibration. This indicates that the stretching vibration of the $–NH_2$ chitosan group has reacted with the epoxide group of GTMAC. A peak at 1095 cm^{-1} revealed the C–O stretching vibration of chitosan. The peak at 2938 cm^{-1} showed the stretching vibration of the $–CH_2–$ or $–CH_3$ groups of chitosan and GTMAC. In addition, the interaction between GTMAC and the $–NH_2$ group is shown with peaks at 1481 cm^{-1}, indicating a quaternary ammonium group, and at 636 cm^{-1}, corresponding C–N–C bending vibration due to the new covalent bond formation between chitosan and GTMAC by epoxide ring opening. On the other hand, the Fe–O stretching vibration peak at 578 cm^{-1}, indicating MM characteristic, was still observed in three samples of various MM/Chit/GTMAC composites (Fig. 1(c), 1(d), and 1(e)). Thus, MM has been successfully coated with quaternary ammonium-modified chitosan.

XRD pattern

XRD patterns of materials are presented in Fig. 2. XRD peaks correspond to magnetite based on the powder diffraction file (PDF) from JCPDS No. 01-075-044 [24]. Peaks 2θ at 30.0, 35.2, 43.0, 54.0, 56.3, and 63.1° correspond to the lattice planes (220), (311), (400), (422), (511), and (440), respectively. There was a significant decrease in the intensity of 2θ peaks of 35.16, 42.82, and 56.70° due to the decline in MM concentration following the addition of chitosan and GTMAC. The presence of chitosan and quaternary ammonium modification affected the crystallinity of MM. The diffractogram shows that with the addition of quaternary ammonium on the MM/Chit, the diffraction pattern of chitosan was getting wider, and the intensity was lower. The broadening of the peaks indicated the heterogeneity of the polymer chains. The peak intensity decreased gradually after the increase in GTMAC concentration. This could be explained by the fact that the quaternary ammonium groups dispersed in the chitosan matrix damaged the chitosan chain. Consequently, the formation of crystal regions was prevented, decreasing the degree of crystallinity [25].

SEM-EDX analysis

From Fig. 3, MM, without modification, exhibits the cubic structure. The surface of MM is smoother than MM/Chit and MM/Chit/GTMAC. The increase in GTMAC concentration caused a denser structure on the

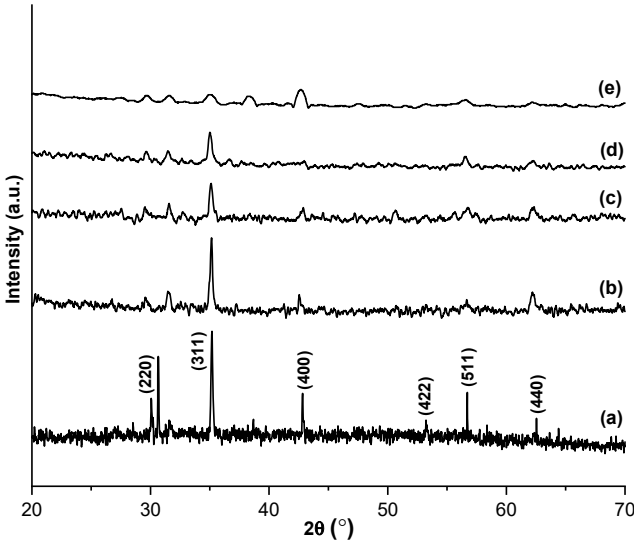

Fig 2. XRD spectra of (a) MM, (b) MM/Chit, (c) MM/Chit/GTMAC(1:2), (d) MM/Chit/GTMAC(1:4), and (e) MM/Chit/GTMAC(1:6)

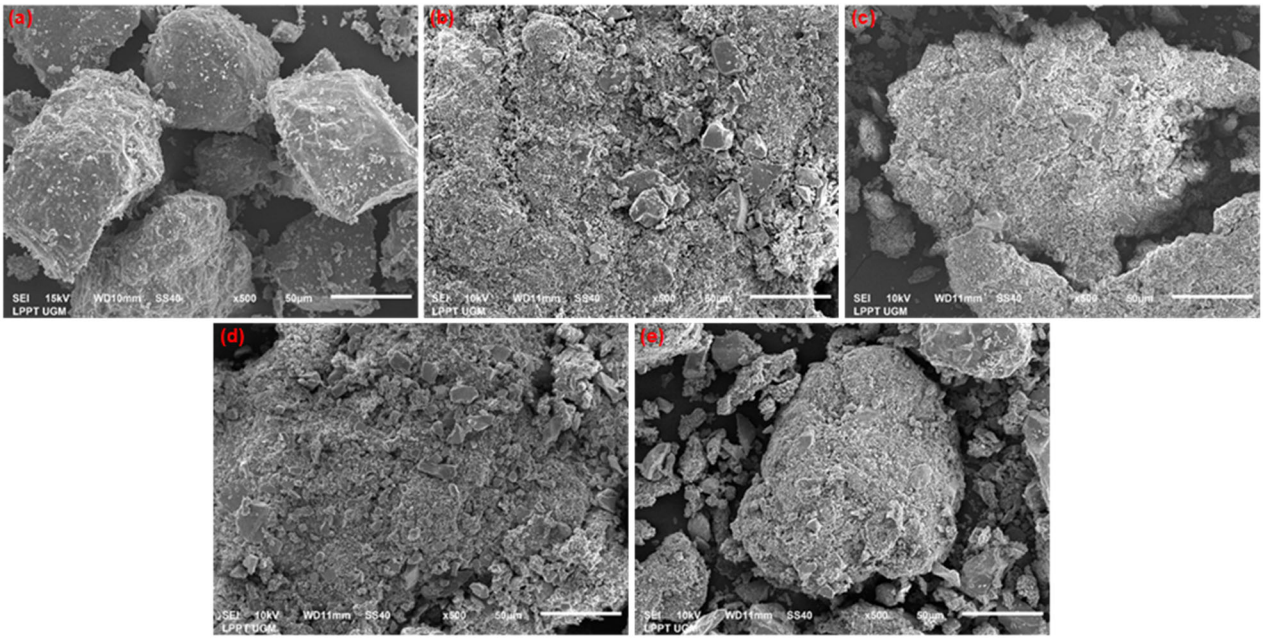

Fig 3. SEM Images of (a) MM, (b) MM/Chit, (c) MM/Chit/GTMAC(1:2), (d) MM/Chit/GTMAC(1:4), and (e) MM/Chit/GTMAC(1:6)

Table 3. EDX Analysis of various MM/Chit/GTMAC

Composite	Element composition (%)				
	C	N	O	Cl	Fe
MM/Chit	15.29	5.99	39.08	0.06	31.38
MM/Chit/GTMAC(1:2)	18.27	6.09	37.38	0.16	31.28
MM/Chit/GTMAC(1:4)	19.09	7.34	37.57	0.28	25.91
MM/Chit/GTMAC(1:6)	25.98	10.36	41.80	1.78	19.05

surface materials. From the EDX analysis shown in Table 3, it is evident that there was a decrease in the percentage of Fe and the addition of C, N, O, and Cl elements from GTMAC after the GTMAC was added to MM/Chit. It indicates that MM was successfully coated with GTMAC-modified chitosan.

Magnetic property

The hysteresis loop of the samples can be observed in Fig. 4. From the hysteresis loop, it appears that there was a decrease in the magnetization value (M_s) of MM after modification. This is because the thicker the coating, the more obstructed MM when approached by an external magnetic field. The modification of the chitosan coating and GTMAC addition would reduce the magnetic properties of the MM due to the more layers coating the MM. As a result, the attraction of the composite by the external magnetic field becomes lower. However, MM/Chit/GTMAC could still be attracted by an external magnet.

pH_{pzc}

The pH_{pzc} for MM/Chit is 6.46, which increased to 7.42 after interacting with GTMAC during the quaternization of a GTMAC composite of MM/Chit

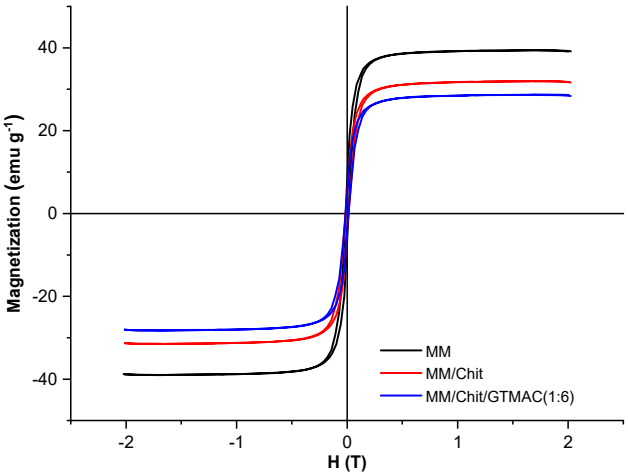

Fig 4. The Hysteresis loop of (a) MM, (b) MM/Chit, (c) MM/Chit/GTMAC(1:6)

(MM/Chit/GTMAC) (Fig. (5)). These results are closely correlated with the pH_{pzc} founded by Zavareh et al. [26], who observed a similar shift in pH_{pzc} after the quaternization process. In this research, the adsorbent was used for the adsorption of Cr(VI) anions where a negative charge was required on the surface of the adsorbent. Based on the pH_{pzc} value obtained, the optimum conditions for adsorption were above pH_{pzc}.

Stability of adsorbents

The stability of MM/Chit and MM/Chit/GTMAC materials was tested by mixing the material with an aqueous solution in the pH range of 1–8. Stability was presented with the amount of Fe released from the material. Fig. 6(a) shows the concentration of iron released for each sample at various pH variations. At pH 1–3, the Fe released from MM/Chit was higher than the three variations of MM/Chit. Furthermore, at pH 2–8, the iron content released from each composite did not differ significantly. The released Fe concentration in MM/Chit/GTMAC(1:6) is the lowest among other composites in the entire pH range. This shows that the MM/Chit/GTMAC(1:6) is the most stable because the MM was coated well with chitosan modified with higher GTMAC. This phenomenon is due to the addition of GTMAC, which can block the protonation of the chitosan amine group so that chitosan does not dissolve easily [27]. In MM/Chit, in an acidic environment, the surface of the uncoated magnetic material comes into direct contact with the acid, which causes high levels of Fe to dissolve after the chitosan dissolves.

Evaluation of product stability based on the concentration of released Fe is supported by chitosan dissolution data using a UV-vis spectrophotometer. Measurements were carried out on the supernatant at maximum absorbance at 282 nm. The absorbance of each sample in varying pH is shown in Fig. 6(b). The

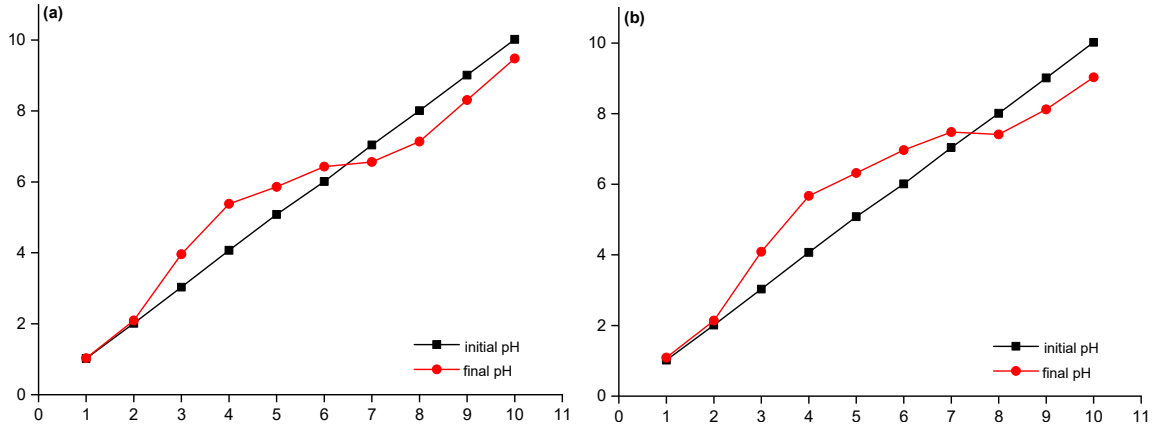

Fig 5. pH_{pzc} curve of (a) MM/Chit and (b) MM/Chit/GTMAC

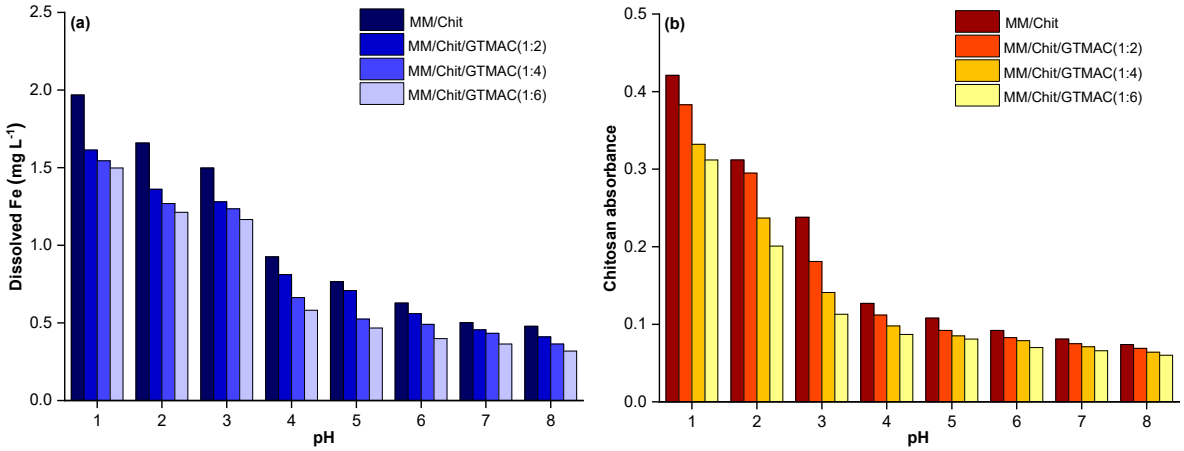

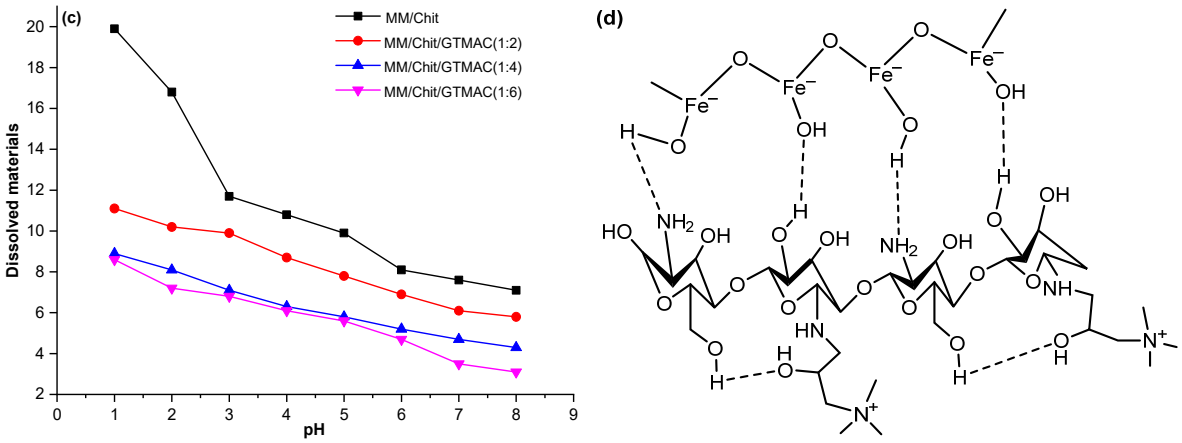

Fig 6. (a) Dissolved Fe, (b) chitosan absorbance, (c) dissolved materials at various pHs, and (d) chemical structure model of MM/Chit/GTMAC

MM/Chit sample gave higher absorbance than MM/Chit/GTMAC at pH 1–3. In this case, MM/Chit/GTMAC(1:6) showed the lowest absorbance value in all pH ranges. This indicates that the more bonds formed between the $-NH_2$ group of chitosan and the epoxy chain of quaternary ammonium, the more stable the synthesized material is against chitosan dissolution.

Dissolved material due to the influence of pH was also measured gravimetrically, and the result is shown in Fig. 6(c). The adsorbent dissolved at various pH values aligns with the dissolved Fe and the UV-vis absorbance of dissolved chitosan. The material dissolved from MM/Chit at pH 1–3 is relatively more than the MM/Chit/GTMAC composite. MM/Chit/GTMAC(1:6) shows the lowest dissolved Fe, chitosan absorbance, and dissolved material in the pH range of 1–8. It shows that the material is the most stable. The stability test indicates that the surface coating of MM with GTMAC-modified chitosan stabilizes the composite under acidic conditions (pH 1–3).

The route of MM/Chit/GTMAC synthesis has been described by Mukhayani et al. [27], and the chemical structure model of the material can seen in Fig. 6(d). In acidic conditions, –Fe–O–Fe– groups on the MM surface react with water molecules to result in two –Fe–OH groups that can form hydrogen bonding with both –C–OH and –C–NH_2 of chitosan or condensation occurs to form –Fe–O–C and –Fe–NH–C by releasing water molecules [28]. The interaction between chitosan and GTMAC occurs due to the opening of epoxy groups by $-NH_2$.

Cr(VI) Adsorption on MM/Chit/GTMAC

pH effect

Fig. 7(a) shows that the adsorption of Cr(VI) anion by MM/Chit increases from pH 1–2 and reaches a maximum at pH 3, then decreases at pH 4. This is because at pH 3 ($pH < pH_{pzc}$), H^+ ions in the solution protonate the $-NH_2$ group in chitosan to $-NH_3^+$. At pH 1, the amount of Cr(VI) anion adsorbed tends to be small, and this is because the Cr(VI) anion is in the form of H_2CrO_4, which is an electroneutral species that is difficult to adsorb. Meanwhile, at pH 3, the most dominant speciation of Cr(VI) in solution was $Cr_2O_7^{2-}$ and $HCrO_4^-$ [29], and the surface charge of MM/Chit was positive. Thus, the adsorption process occurred optimally. The protonated $-NH_2$ group acts as a Lewis acid capable of absorbing Cr(VI) anions in solution through electrostatic interactions [30]. This electrostatic force causes Cr(VI) to be adsorbed by the MM/Chit adsorbent. Increasing pH causes a decrease in adsorption activity. It is possible because all of the active sites of the adsorbent are not protonated completely, so the interaction between the adsorbent and the adsorbate is weaker. Adsorption occurs probably due to electrostatic interaction, as presented in Eq. (3) for MM/Chit and Eq. (4) for MM/Chit-GTMAC.

$$[-NH_3]^+ + [HCrO_4]^- \rightarrow [-NH_3]^+[HCrO_4]^- \quad (3)$$

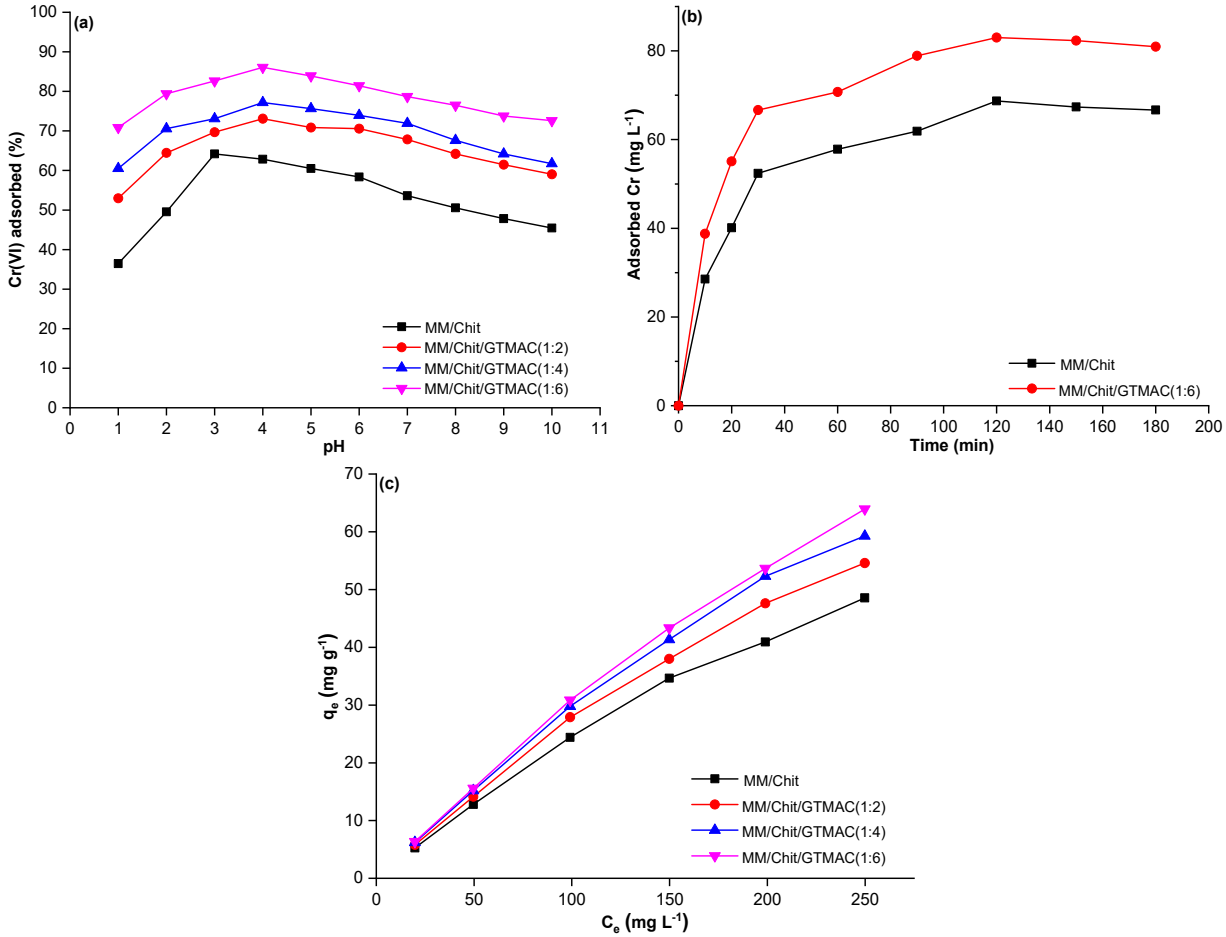

Fig 7. Effect of (a) pH, (b) time, and (c) equilibrium concentration on Cr(VI) adsorption

$$[-N(CH_3)_3]^+ + [HCrO_4]^- \rightarrow [N(CH_3)_3]^+[HCrO_4]^- \quad (4)$$

The adsorption of Cr(VI) anions on the MM/Chit/GTMAC(1:2), MM/Chit/GTMAC(1:4), and MM/Chit/GTMAC(1:6) composites showed that the adsorption increased from pH 1–3 and reached a maximum at pH 4, then decreased at pH 5. There was a shift in the optimum pH compared to MM/Chit, which gave optimum results at pH 3. This is because the pH_{pzc} of MM/Chit/GTMAC was higher than that of MM/Chit, which shows that the surface charge of the adsorbent was still positive, along with the increase in pH. In line with the positive charge of GTMAC, namely $-(N(CH_3)_3)^+$ was not affected by pH. This causes a shift to a higher optimum pH given by MM/Chit/GTMAC. At pH 1, the amount of Cr(VI) anion absorbed by the three composites of MM/Chit/GTMAC tended to be small. There is no significant difference with the optimum condition of MM/Chit because Cr(VI) anion in H_2CrO_4 causes a small adsorption percentage. The presence of the $-(N(CH_3)_3)^+$ group of GTMAC can adsorb Cr(VI) metal in solution through electrostatic interactions [31]. The increase in pH causes the adsorption to decrease but remains stable when compared to MM/Chit because of a quaternary group in MM/Chit/GTMAC. In this research, MM/Chit/GTMAC(1:6) has the highest adsorption (86.1%).

Adsorption kinetics

The kinetics was evaluated based on the data of Cr(VI) adsorption at various times, and the result is expressed in Fig. 7(b). Kinetics parameters can be determined using two models presented in Table 2, and the results are summarized in Table 4. It can be seen that the adsorption of Cr(VI) on MM/Chit and MM/Chit/GTMAC(1:6) followed the pseudo-second-

order kinetic model. The chemisorption involves the formation of a strong bond between Cr(VI) ions with MM/Chit and MM/Chit/GTMAC(1:6) composites and forms a monolayer on the surface of the adsorbent. Therefore, the adsorption capacity is equivalent to the active site of the adsorbent. Pseudo-second-order kinetics is a kinetic model described in two stages: a fast initial stage and a slower second stage [32]. This follows the research results on the effect of variations in contact time on Cr(VI) adsorption shown in Fig. 7(b). The trend shows that in the initial stage, a fast reaction occurs because the concentration of adsorbed Cr(VI) increases with increasing contact time to a maximum point. The second stage is a slower reaction, as evidenced by the decrease in the adsorption of Cr(VI) anions by the adsorbent after the optimum time has passed.

Adsorption isotherm

The adsorption capacity of the Cr(VI) anion over the adsorbent was determined using the adsorption isotherm. The adsorption isotherm pattern was studied by interacting several composites with Cr(VI) solutions of various concentrations at optimum pH and time. Determination of the optimum concentration was carried out at pH 3 for MM/Chit and pH 4 for MM/Chit/GTMAC with a contact time of 120 min using 50 mg of composite. The optimum concentration was determined with a volume of 20 mL and various Cr(VI) concentrations of 20, 50, 100, 150, 200, and 250 ppm. The result is presented in Fig. 7(c). The higher initial concentration of adsorbate provides a greater driving force so that Cr(VI) will migrate from the solution to the active site of the adsorbent. It can be seen that the adsorption capacity of MM/Chit/GTMAC(1:6) is greater than that of MM/Chit, MM/Chit/GTMAC(1:2), and MM/Chit/GTMAC(1:4). It can be understood that higher GTMAC added leads to the increase of the quaternary ammonium number and the adsorption capacity increase accordingly. It is supported by the highest nitrogen content in MM/Chit/GTMAC(1:6), as presented in Table 3. When the concentration reaches equilibrium, the amount of adsorbate adsorbed relatively does not increase even though the initial concentration of adsorbate is increased. This indicates that the active sites on the adsorbent have been saturated by Cr(VI) and have reached their adsorption capacity.

Langmuir and Freundlich isotherm model parameters for Cr(VI) adsorption over MM/Chit, MM/Chit/GTMAC(1:2), MM/Chit/GTMAC(1:4), and MM/Chit/GTMAC(1:6) shown in Table 5. Based on the R^2 value closest to one, the Cr(VI) adsorption isotherm over the adsorbent followed the Langmuir isotherm model. This shows that the surface active side of the adsorbents is homogeneous, so the adsorption of Cr(VI) ions on the four composites only forms one layer (monolayer). This indicates that only one group was dominant in adsorbing Cr(VI) ions. A comparison of the adsorption capacity of MM/Chit and MM/Chit/GTMAC in this study with other adsorbents is shown in Table 6.

Table 4. Parameters of Cr(VI) adsorption kinetics

Adsorbent	Pseudo-first-order		Pseudo-second-order	
	k_1 (min^{-1})	R^2	k_2 (g mg^{-1} min^{-1})	R^2
MM/Chit	2.89×10^{-5}	0.707	4.90×10^{-3}	0.996
MM/Chit/GTMAC(1:6)	3.61×10^{-5}	0.778	5.30×10^{-3}	0.998

Table 5. Adsorption isotherm parameter of Cr(VI) on the composites

Adsorbent	Langmuir parameter		Freundlich parameter	
	R^2	q_{max} (mg g^{-1})	R^2	K_F (L g^{-1})
MM/Chit	0.991	85.47	0.986	2.208
MM/Chit/GTMAC(1:2)	0.989	91.74	0.981	4.453
MM/Chit/GTMAC(1:4)	0.993	95.23	0.980	7.954
MM/Chit/GTMAC(1:6)	0.990	104.17	0.981	9.143

Table 6. Comparison of the Cr(VI) adsorption capacity on MM/Chit and MM/Chi/GTMAC to other adsorbents

Adsorbent	q_{max} (mg g^{-1})	Reference
Activated carbon	71.86	[33]
Chitosan-alumina	66.90	[34]
Chitosan fiber	75.00	[30]
Chitosan-GO-α-FeO(OH)	63.15	[35]
Chitosan-humic acid-GO	83.64	[36]
MM/Chit	85.47	This study
MM/Chit/GTMAC	104.17	This study

Apart from the highest adsorption capacity for Cr(VI), another advantage of the MM/Chit/GTMAC is that it can be easily recovered using an external magnetic field. The MM/Chit/GTMAC has excellent potential to be developed as a low-cost and environmentally friendly adsorbent because it uses non-toxic materials and is very easy to obtain from nature. Therefore, MM/Chit/GTMAC can be an alternative adsorbent candidate to remove Cr(VI) pollutants from aquatic environments.

■ CONCLUSION

The MM coating using GTMAC-modified chitosan produced a positively charged MM/Chit/GTMAC adsorbent that can be used to adsorb Cr(VI) anion. Cr(VI) adsorption on MM/Chit/GTMAC(1:6) was optimum at pH 4 with an adsorption capacity of 86.1%. The adsorption process of Cr(VI) anion over MM/Chit/GTMAC(1:6) followed the pseudo-second-order kinetics and Langmuir adsorption isotherm models with the adsorption rate constant and the adsorption capacity of 5.3×10^{-3} g mg^{-1} min^{-1} and 104.17 mg g^{-1}, respectively. This adsorbent can potentially remove Cr(VI) from the aquatic environment.

■ ACKNOWLEDGMENTS

Part of the paper has been orally presented at the International Conference of the Indonesian Chemical Society (ICICS) 2023, supported by Universitas Gadjah Mada with contract number 6324/UN1/DITLIT/Dit-Lit/PL.01.05/2023.

■ CONFLICT OF INTEREST

There are no conflicts of interest to declare.

■ AUTHOR CONTRIBUTIONS

Salwa Kamilia: Methodology, Investigation, Data visualization, Writing-original draft; Feri Mukhayani: Data visualization and writing-editing. Nuryono and Sutarno: Conceptualization, Formal analysis, Writing-review and Editing. All authors have approved the final version of the manuscript.

■ REFERENCES

[1] Sun, H., Brocato, J., and Costa, M., 2015, Oral chromium exposure and toxicity, *Curr. Environ. Health Rep.*, 2 (3), 295–303.

[2] Fang, Y., Yang, K., Zhang, Y., Peng, C., Robledo-Cabrera, A., and López-Valdivieso, A., 2021, Highly surface activated carbon to remove Cr(VI) from aqueous solution with adsorbent recycling, *Environ. Res.*, 197, 111151.

[3] Mishra, S., and Bharagava, R.N., 2016, Toxic and genotoxic effects of hexavalent chromium in environment and its bioremediation strategies, *J. Environ. Sci. Health, Part C: Environ. Carcinog. Ecotoxicol. Rev.*, 34 (1), 1–32.

[4] Li, Y.H., Liu, M.Y., Wei, Y.W., Wang, C.C., and Wang, P., 2023, Adsorption and photocatalytic desorption toward Cr(VI) over defect-induced hierarchically porous UiO-66-$(OH)_2$: A sustainable approach, *Environ. Sci.: Nano*, 10 (2), 672–682.

[5] El Gaayda, J., Rachid, Y., Titchou, F.E., Barra, I., Hsini, A., Yap, P.S., Oh, W.D., Swanson, C., Hamdani, M., and Akbour, R.A., 2023, Optimizing removal of chromium(VI) ions from water by coagulation process using central composite design: Effectiveness of grape seed as a green coagulant, *Sep. Purif. Technol.*, 307, 122805.

[6] Sellami, F., Kebiche-Senhadji, O., Marais, S., Colasse, L., and Fatyeyeva, K., 2020, Enhanced removal of Cr(VI) by polymer inclusion membrane based on poly(vinylidene fluoride) and Aliquat 336, *Sep. Purif. Technol.*, 248, 117038.

[7] Liu, M., Wang, Y., Wu, Y., Liu, C., and Liu, X., 2023, Sol-gel synthesis of magnesium aluminate and synergistic degradation of Cr(VI) ion by adsorption and photocatalysis, *Front. Mater.*, 10 (10), 1274625.

[8] Shah, S., Mubeen, I., Pervaiz, E., and Nasir, H., 2023, Enhanced removal of toxic Cr(VI) and Pb(II) from water using carboxylic terminated $Ti_3C_2T_x$ nanosheets, *RSC Adv.*, 13 (33), 23320–23333.

[9] Fallah, Z., and Roberts, E.P.L., 2019, Combined adsorption/regeneration process for the removal of trace emulsified hydrocarbon contaminants, *Chemosphere*, 230, 596–605.

[10] Li, W., Chai, L., Du, B., Chen, X., and Sun, R.C., 2023, Full-lignin-based adsorbent for removal of Cr(VI) from waste water, *Sep. Purif. Technol.*, 306, 122644.

[11] Akl, M.A., Mostafa, A.G., Abdelaal, M.Y., and Nour, M.A.K., 2023, Surfactant supported chitosan for efficient removal of Cr(VI) and anionic food stuff dyes from aquatic solutions, *Sci. Rep.*, 13 (1), 15786.

[12] Hezma, A.M., Shaltout, W.A., Kabary, H.A., El-Bahy, G.S., and Abdelrazzak, A.B., 2023, Fabrication, characterization and adsorption investigation of nano zinc oxide–sodium alginate beads for effective removal of chromium(VI) from aqueous solution, *J. Inorg. Organomet. Polym. Mater.*, 33 (5), 1400–1408.

[13] Li, Q., Huang, Q., Pan, X.Y., Yu, H., and Zhao, Z.T., 2022, Adsorption behavior of Cr(VI) by biomass-based adsorbent functionalized with deep eutectic solvents (DESs), *BMC Chem.*, 16 (1), 41.

[14] Wang, K., Zhang, F., Xu, K., Che, Y., Qi, M., and Song, C., 2023, Modified magnetic chitosan materials for heavy metal adsorption: A review, *RSC Adv.*, 13 (10), 6713–6736.

[15] Budnyak, T.M., Pylypchuk, I.V., Tertykh, V.A., Yanovska, E.S., and Kolodynska, D., 2015, Synthesis and adsorption properties of chitosan-silica nanocomposite prepared by sol-gel method, *Nanoscale Res. Lett.*, 10 (1), 87.

[16] Khapre, M.A., and Jugade, R.M., 2022, Quaternary ammonium impregnated chitosan for the decontamination of wastewater from carcinogenic dyes, *Environ. Processes*, 9 (2), 24.

[17] Woźniak, A., and Biernat, M., 2022, Methods for crosslinking and stabilization of chitosan structures for potential medical applications, *J. Bioact. Compat. Polym.*, 37 (3), 151–167.

[18] Ibrahim, A.G., Elgammal, W.E., Eid, A.M., Alharbi, M., Mohamed, A.E., Alayafi, A.A.M., Hassan, S.M., and Fouda, A., 2023, New functionalized chitosan with thio-thiadiazole derivative with enhanced inhibition of pathogenic bacteria, plant threatening fungi, and improvement of seed germination, *Chemistry*, 5 (3), 1722–1744.

[19] Rwei, S.P., Chen, Y.M., Lin, W., and Chiang, W.Y., 2014, Synthesis and rheological characterization of water-soluble glycidyltrimethylammonium-chitosan, *Mar. Drugs*, 12 (11), 5547–5562.

[20] Gruškienė, R., Deveikytė, R., and Makuška, R., 2013, Quaternization of chitosan and partial destruction of the quaternized derivatives making them suitable for electrospinning, *Chemija*, 24 (4), 325–334.

[21] Li, Z., Yang, C., Qu, G., Cui, Q., Yang, Y., Ren, Y., Yang, Y., and Wang, F., 2023, Chitosan-modified magnetic carbon nanomaterials with high efficiency, controlled motility, and reusability—for removal of chromium ions from real wastewater, *Environ. Sci. Pollut. Res.*, 30 (17), 51271–51287.

[22] Nuryono, N., Rosiati, N.M., Rusdiarso, B., Sakti, S.C.W., and Tanaka, S., 2014, Coating of magnetite with mercapto modified rice hull ash silica in a one-pot process, *SpringerPlus*, 3 (1), 515.

[23] El-Naggar, N.E.A., Shiha, A.M., Mahrous, H., and Mohammed, A.B.A., 2022, Green synthesis of chitosan nanoparticles, optimization, characterization and antibacterial efficacy against multi drug resistant biofilm-forming *Acinetobacter baumannii*, *Sci. Rep.*, 12 (1), 19869.

[24] Denison, M.I.J., Raman, S., Duraisamy, N., Thangavelu, R.M., Riyaz, S.U.M., Gunasekaran, D., and Krishnan, K., 2015, Preparation, characterization and application of antibody-conjugated magnetic nanoparticles in the purification of begomovirus, *RSC Adv.*, 5 (121), 99820–99831.

[25] Mivehi, L., Bahrami, S.H., and Malek, R.M.A., 2008, Properties of polyacrylonitrile-*N*-(2-hydroxy) propyl-3-trimethylammonium chitosan chloride blend films and fibers, *J. Appl. Polym. Sci.*, 109 (1), 545–554.

[26] Zavareh, S., Avanes, A., and Beiramyan, P., 2017, Effective and selective removal of aromatic amines

from water by Cu^{2+}-treated chitosan/alumina nanocomposite, *Adsorpt. Sci. Technol.*, 35 (1-2), 218–240.

[27] Mukhayani, F., Kamiya, Y., Otomo, R., Kunarti, E.S., and Nuryono, N., 2024, Modification of chitosan-coated magnetic material with glycidyltrimethylammonium chloride and its application as heterogeneous base catalyst for levulinic acid esterification, *Mater. Adv.*, 5 (9), 3838–3849.

[28] Mukhayani, F., Kunarti, E.S., Kamiya, Y., and Nuryono, N., 2024, Preparation and characterization of magnetic material/chitosan composite modified with glycidyl-trimethylammonium chloride, *Indones. J. Chem.*, 24 (2), 444–458.

[29] Balan, C., Volf, I., and Bilba, D., 2013, Chromium(VI) removal from aqueous solutions by Purolite base anion-exchange resins with gel structure, *Chem. Ind. Chem. Eng. Q.*, 19 (4), 615–628.

[30] Zhang, S., Zhang, Y., Fu, L., and Jing, M., 2021, A chitosan fiber as green material for removing Cr(VI) ions and Cu(II) ions pollutants, *Sci. Rep.*, 11 (1), 22942.

[31] Sun, X., Li, Q., Yang, L., and Liu, H., 2016, Removal of chromium(VI) from wastewater using weakly and strongly basic magnetic adsorbents: Adsorption/desorption property and mechanism comparative studies, *RSC Adv.*, 6 (22), 18471–18482.

[32] Shahnaz, T., Patra, C., Sharma, V., and Selvaraju, N., 2020, A comparative study of raw, acid-modified and EDTA-complexed *Acacia auriculiformis* biomass for the removal of hexavalent chromium, *Chem. Ecol.*, 36 (4), 360–381.

[33] Kumar, A., and Jena, H.M., 2016, Preparation and characterization of high surface area activated carbon from Fox nut (*Euryale ferox*) shell by chemical activation with H_3PO_4, *Results Phys.*, 6, 651–658.

[34] Darjito, D., Purwonugroho, D., and Ningsih, R., 2014, The adsorption of Cr(VI) ions using chitosan-alumina adsorbent, *J. Pure Appl. Chem. Res.*, 3 (2), 53–61.

[35] Liu, Y., Shan, H., Zeng, C., Zhan, H., and Pang, Y., 2022, Removal of Cr(VI) from wastewater using graphene oxide chitosan microspheres modified with α–FeO(OH), *Materials*, 15 (14), 4909.

[36] Parlayıcı, Ş., Avcı, A., and Pehlivan, E., 2019, Fabrication of novel chitosan-humic acid-graphene oxide composite to improve adsorption properties for Cr(VI), *Arabian J. Geosci.*, 12 (19), 615.